LASER INTERFEROMETER GRAVITATIONAL WAVE OBSERVATORY
- LIGO -
==========
LIGO LABORATORY

Technical Note **LIGO-T2400167–v2** 2024/06/03

Updated model of the D-R isotherm applied to large UHV vacuum systems based on the framework originally developed by R. Weiss for iLIGO

A. Lazzarini, J. Feicht

Distribution of this document:
LIGO Laboratory

http://www.ligo.org/

Contents

List of Figures

1 Summary

This document describes modifications made to the original R. Weiss FORTRAN code developed to model the outgassing properties of the initial LIGO beamtubes [1] and which has now been ported to Mathematica™.

In the 1990s R. Weiss developed an adsorption isotherm computer model to predict water outgassing from the LIGO beamtubes. The model uses Langmuir theory with a Dubinin-Raduskevich (D-R) distribution of absorption site binding energies as a canonical ensemble. The model includes a (re)adsorption potential, given as a fraction of the desorption energy, which controls the readsorption rate and prevents the outgassed species from immediately being readsorbed. The desorption energy range was selected based on sojourn times and outgassing data; a peak energy of $\sim$ 1 eV (about 24 kcal/mole) was found to match the stainless steel used for beamtube construction. The model parameters were calibrated against outgassing data from a 40m long test section of beamtube.

The code predicts the surface outgassing rate, which is converted into a pressure distribution by a 1-d Knudsen flow equation. A typical analysis breaks the problem into 20 to 100 sections, with a Runge-Kutta algorithm solving the coupled differential equations for the pressure distribution. A variety of parameters such as pump distribution, leaks, temperature, etc. are included in the model and can be switched on/off at various times to simulate bakeouts, valve modulation, vacuum leaks, etc. The code runs for a fixed total time, looping through the various parameters and creating a pressure versus time profile. A copy of the FORTRAN source code is archived in the DCC [2], and can be opened with a text reader.

In 2018 LIGO Engineering management requested that the dormant FORTRAN code be reconstituted with a high-level programming language, e.g., MatLab™ or Mathemetica™ rather than simply recompiled with an updated FORTRAN release. These high-level codes are actively developed, have optimized differential equation and matrix solvers, and include advanced graphics capabilities. This effort initially resulted in a Mathematica™ transcription of the code that closely followed the FORTRAN structure. Although operable, these early releases were hampered by copying the nested looping constructs of the original code, resulting in long solve times.

This document describes a series of modifications made to the Mathematica™ code to speed up the solve time. Much of the original FORTRAN structure was replaced by native Mathematica™ functions for the manipulation of matrices and arrays [3]. These modifications increased the code performance to allow many-week runs starting with an initial step size set by the system time constant, $\sim \frac{volume}{(pumpingspeed)}$.

Some of the improvements that were introduced.

- The pump arrangements, leaks, temperature profile, etc. can be defined along the beamtube.
- The D-R isotherm was originally developed to model pores, for example activated carbon which has extensive surface area. This is different than Langmuir isotherms that model surface coverage layers (unity and often $<$ 1 layer). Consequently, good reproduction of actual pump down data will typically require » 1 layer. Multiple water

layers have a low sticking probability, so this parameter is better associated with an equivalent surface roughness.

- The D-R function that determines surface outgassing rate, probev[], now uses native Mathematica language structures to efficiently carry out the nested do loops in the original FORTRAN code.
- Reformulated the discrete Laplacian as a tridiagonal matrix to generate the differential equations. This eliminated additional do-loops and further improved performance.
- Introduced the ability to define surface temperature by each element of the beamtube; elements (sections) are defined to calculate the spatial derivatives for the PDE. Typically 40 - 100 sections are implemented. This defines the dimensionality of the PDE and size of Laplacian matrix.
- The state of a calculation can be written to file as a native Mathematica .mx file. Note that these files can be up to 10+GB in size. Rereading the file in a later session allows one to start off where one left off earlier.
- Introduced the ability to specify a sequence of bake events by specifying transition times, duration and temperature. Can also introduce leaks that appear and disappear vs. time.
- Added ability to view the time dependent probability of the bound (surface) water population ap[x,t].
- Turned a number of thermodynamic values into temperature-dependent thermodynamic functions to allow for updating during the bake sequencing. Same with the diffusion constant.
- Modified the diffusion constant per LM Lund & AS Berman[4] which provides a smooth transition from free molecular regime to viscous regime. This allows runs to start at 20 Torr (the water vapor partial pressure at atmospheric pressure).
- Added a convection term to the diffusion equation to allow studies of sectional bakes in the presence of a dry inert gas (air or N_2) to entrain the outgassed H_2O vapor and remove it from the tube.

2 Introduction

The partial differential equation (PDE) to be solved is the time dependent diffusion equation with source (leaks, $q_{lk}(x,t)$, and outgassing, $a_{jj}(x,t)$) and sink (pumping, $S(x)p(x,t)$) terms. Modeling a system that has a continuous flow of background dry inert gas flowing at velocity V to entrain the outgassing H_2O can be done by using the diffusion-convection equation[1].

[1]The general convection term assumes a spatially dependent velocity: $\nabla_x(V(x)p(x,t))$, which allows for compressible flow. The expression in Eq.1 is termed the non-conservative form that assumes a constant V. In general (per Mathematica docuentation on mass transport PDEs), the non-conservative formulation is appropriate for situations in which the variation with position of $p(x,t)$ is expected to be smooth.

Because the beamtube aspect ratio, $\frac{length}{diameter} \gg 1$, it is sufficient to consider a PDE with one spatial dimension. Then the equation may be written as:

$$\frac{\partial p(x,t)}{\partial t} = \underbrace{D(T)\nabla_x^2 p(x,t)}_{\text{diffusion}} - \underbrace{V\nabla_x p(x,t)}_{\text{convection}} + \underbrace{b a_{jj}(x,t)}_{\text{outgassing}} + \underbrace{d(q_{lk}(x,t)}_{\text{leaks}} - \underbrace{S(x,t)p(x,t))}_{\text{pumping}} \quad (1)$$

2.1 Discretized form of the PDE

Discretizing in x, $x_i \rightarrow i\ \delta L$ with i=$\{0$,..., $N_{segments}\}$ and $p(x_i,t) \rightarrow p_i(t)$, then Eq. 1 can be written as

$$\frac{\partial p_i(t)}{\partial t} = \mathbf{D}(T)(p_i(t)+p_{i-2}(t)-2p_{i-1}(t))+ba_{jj}(x,t)-V(p_i(t)-p_{i-1}(t))+d(q_{lk}(i,t)-S(i,t)p_i(t)) \quad (2)$$

Eq. 2 can be efficiently represented by a matrix of coupled differential equations involving a tridiagonal matrix for the Lapalacian operator ∇_x^2 and an bidiagonal matrix for the gradient operator ∇_x:

$$\nabla_x^2\ p(x,t) \rightarrow \begin{bmatrix} -1 & 1 & 0 & 0 & 0 & 0 & \cdots & 0 & 0 \\ 1 & -2 & 1 & 0 & 0 & 0 & \cdots & 0 & 0 \\ 0 & 1 & -2 & 1 & 0 & 0 & \cdots & 0 & 0 \\ 0 & 0 & 1 & -2 & 1 & 0 & \cdots & 0 & 0 \\ 0 & 0 & 0 & 1 & -2 & 1 & \cdots & 0 & 0 \\ \vdots & \vdots & \vdots & \vdots & \vdots & \vdots & \vdots\vdots\vdots & \vdots & \vdots \\ 0 & 0 & 0 & 0 & 0 & 1 & -2 & 1 & 0 \\ 0 & 0 & 0 & 0 & 0 & 0 & 1 & -2 & 1 \\ 0 & 0 & 0 & 0 & 0 & 0 & 0 & 1 & -1 \end{bmatrix} \cdot \begin{bmatrix} p_1(t) \\ p_2(t) \\ p_3(t) \\ p_4(t) \\ p_5(t) \\ \vdots \\ p_{N-2}(t) \\ p_{N-1}(t) \\ p_N(t) \end{bmatrix} \quad (3)$$

and

$$\nabla_x\ p(x,t) \rightarrow \begin{bmatrix} -1 & 1 & 0 & 0 & 0 & 0 & \cdots & 0 & 0 \\ 0 & -1 & 1 & 0 & 0 & 0 & \cdots & 0 & 0 \\ 0 & 0 & -1 & 1 & 0 & 0 & \cdots & 0 & 0 \\ 0 & 0 & & -1 & 1 & 0 & \cdots & 0 & 0 \\ 0 & 0 & 0 & & -1 & 1 & \cdots & 0 & 0 \\ \vdots & \vdots & \vdots & \vdots & \vdots & \vdots & \vdots\vdots\vdots & \vdots & \vdots \\ 0 & 0 & 0 & 0 & 0 & 0 & -1 & 1 & 0 \\ 0 & 0 & 0 & 0 & 0 & 0 & 0 & -1 & 1 \\ 0 & 0 & 0 & 0 & 0 & 0 & 0 & 0 & 0 \end{bmatrix} \cdot \begin{bmatrix} p_1(t) \\ p_2(t) \\ p_3(t) \\ p_4(t) \\ p_5(t) \\ \vdots \\ p_{N-2}(t) \\ p_{N-1}(t) \\ p_N(t) \end{bmatrix} \quad (4)$$

2.2 Parameters of the PDE

2.2.1 Diffusion constant, D(T)

The diffusion constant is given by

$$\mathbf{D}(T) = \frac{1}{SectionLength^2}\Big(\frac{2}{3}v_{mean}[T, M_{H_2O}]\frac{TubeID}{2}\Big)\Big(\frac{1}{1 + TubeID/\lambda_{Mean}[P_{N_2}, T]}\Big). \quad (5)$$

The factor $\frac{1}{SectionLength^2}$ arises from the discretization of ∇_x^2. The last term provides a smooth transition between free streaming molecular flow in the UHV regime ($\lambda_{mean} \gg TubeID$) when the beamtube geometry determines mean free path, and laminar viscous flow, when the small mean free path dominates ($\lambda_{mean} \ll TubeID$).

2.2.2 Convection term, $V\nabla_x p(x,t)$

A full-length bakeout of a system on the scale of the 80-km of beamtube envisioned for Cosmic Explorer (CE) is not possible in the manner carried out for initial LIGO. Instead a moving inductive heating of a much shorter (∼1 m) section of beamtube is being explored as an alternative approach. The idea is to continuously flow a dry, inert gas (e.g., air or N_2) at low pressure down the length of the beamtube to entrain and remove the outgassed H_2O from the section under bake. The issue is whether back-diffusion of the outgassed H_2O upstream, against the dry gas flow will repopulate the surface sites that were previously depleted. To study this, a convective term is included in the diffusion equation.

Convective migration of a dilute substance in the presence of a background flow of a second substance is a well-studied mass transport process in a number of fields, e.g., ecology, biophysics and semiconductor physics. It was first investigated over a century ago by M. Smoluchowski[5], after whom the convection (or drift)-diffusion equation is named (see also [6][7]).

The simplest model assumes a constant background flow field V of transport gas into which the outgassing H_2O vapor is entrained and carried away. The efficacy of convection is proportional to the pressure gradient of H_2O vapor.

2.2.3 Outgassing, $b \cdot a_{jj}(x,t)$

The outgassing term follows from the D-R isotherm implementation by R. Weiss in the early 1990s and documented in a number of technical notes in the LIGO DCC[1] as referenced above. The coefficient b is determined by the beamtube geometry.

2.2.4 Leaks, $d \cdot q_{lk}(x,t)$

Leaks can be introduced at different locations and can be turned on or off. This was useful in the original initial LIGO modeling to identify leaks that developed over time along the 4 km arms. It was used to develop a strategy for localizing leaks. The coefficient d is determined by the beamtube geometry.

2.2.5 Pumping, $d \cdot S(x,t) \cdot p(x,t)$

The gas removal rate is given by pumping speed, $S(x,t)$, times the pressure at the pump port, $p(x,t)$. The coefficient d is the same as the one for leaks and is determined by the beamtube geometry.

3 Details

The Mathematica code allows rapid calculation of the pressure profile over very long time spans. This is possible because the spacing of the points in time when the PDE is evaluated can grow progressively as time evolves. After initial transients whose time scale is determined by the system time constant, $\sim \frac{volume}{(pumpingspeed)}$, the asymptotic behavior becomes $p(t) \sim t^{-\alpha}$, which lends itself to geometrically increasing time steps without loss of accuracy. For example, the implementation shown in Fig. 1 starts each bakeout with a 1s timestep that then grows $\sim 200\times$ over the course of a bake. Refer to the figure caption for details. The case shown is for a series of 40 bakeouts, each lasting 0.25 days, followed by a pumpdown at room temperature lasting 5 days: a 1.3×10^6s time span is covered with $\sim 2 \times 10^4$ time steps.

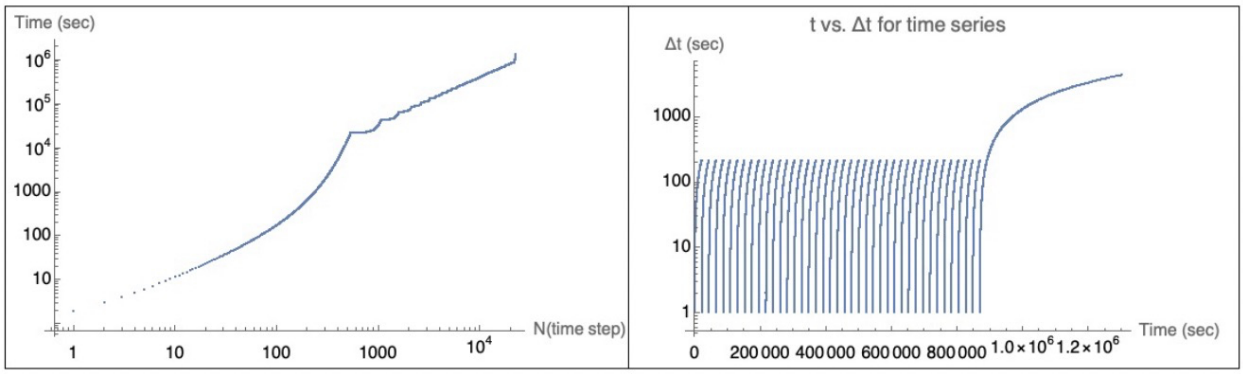

Figure 1: *By logarithmically spacing the times when the PDE is numerically solved, it is possible to calculate the pressure evolution over very long time spans efficiently: since the asymptotic behavior is $p(t) \sim t^{-\alpha}$, the time steps can be increased without loss of accuracy. Left panel: the time span (on ordinate) $[1s, 2 \times 10^6 s]$ is covered by $\sim 2 \times 10^4$ steps of increasing size. Right panel: time step Δt vs. t when the PDE is calculated. Each bakeout starts with the smallest time step that then increases with time.*

The code allows for arbitrary distributed pumping and presence of leaks. Fig. 2 shows an example run for a configuration with end pumping by 160 l/s turbopumps and with no leaks along the length of the beamtube.

Fig. 3 shows the allocation of 1024 sites to binding energies spanning the range [0, 30kK] and the corresponding D-R weighting function used to model the characteristics of H_2O adsorption and desorption.

3.1 Model calibration on data

The D-R model was compared against two datasets: pumpdown and bake data kindly provided by C. Scarcia from CERN for their ET prototype test and LTREX room temeprature pumpdown performed at Caltech.

3.1.1 CERN ET prototype comparison

Fig. 4 shows the pumpdown curve for the D-R model comparing it to CERN prototype data shared with Caltech by C. Scarcia. The system was pumped down at room temperature (20C)

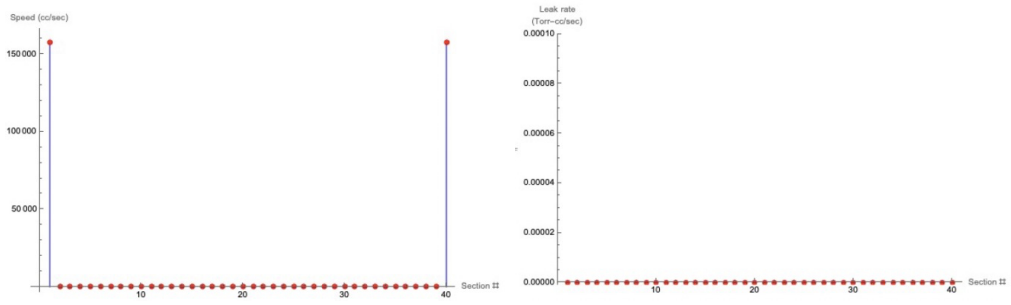

Figure 2: *Left panel: Schematic of pumping arrayed along the 40 sections of the beamtube. In this example two turbos provide end pumping of* $\sim$ *160*$\times 10^3$*cc/sec (*$\sim$*160 l/sec) each. Right panel: Schematic of leaks arrayed along the 40 sections of the beamtube. In this example all leaks were set to 0.*

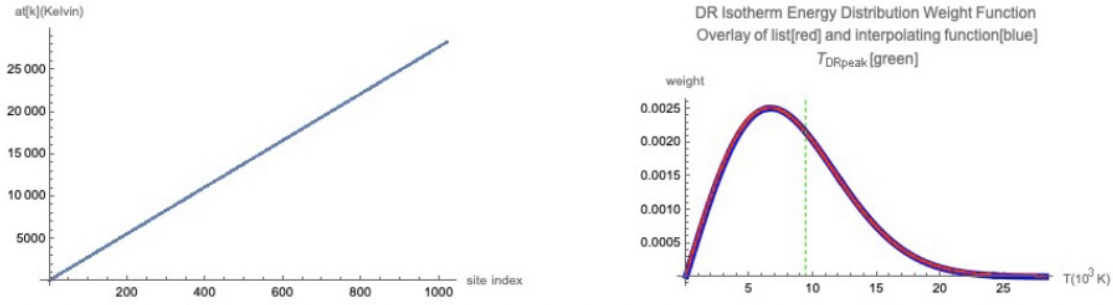

Figure 3: *The Dubinin-Radushkevich (D-R) isotherm. Left panel: allocation of 1024 energy sites to binding energies (measured in K) from 0K to* $\sim$ *30kK. Right panel: weighting function that goes into the D-R model to assign occupation probability of energy sites. The green vertical line corresponds to the parameter* $T_{DR-peak}$ *of the model, here set to* $\sim$*9.4kK.*

for about 18 days; data are not available for a significant portion of this initial pumpdown. Then the temperature was raised to 80C for 7 days. It was not clear whether the 1mm or 10mm orifice was used for different portions of the 7 day bakeout. However based on exploration with the model using different orifice configurations, the quality of fit shown suggests that for the first 2 days pumping was through the 1mm orifice, then for the remaining 5 days pumping was through the 10mm orifice: using only either the 1mm orifice pumping or the 10mm orifice pumping gave results that are unlike the data. Additional details are provided in the figure caption.

In order to get the fit shown in Fig. 4 the following D-R parameters were varied: $0 \leq \alpha \leq 1$(accommodation coefficient); T_{DRpeak} that scales the binding energy distribution of energies of the sites; and σ_0 (initial surface loading – essentially the # of monolayers on the surface prior to pumpdown). Fig. 5 shows the dependence of the fractional RMS deviation between the D-R model and the CERN data as these parameters are varied. The fractional RMS was calculated for the bakeout portion of the data, leaving out the rapid ramp-up and ramp-down transients and the beginning and end of the 2-day part of the bakeout. The transient at the end of the bakeout was also omitted.

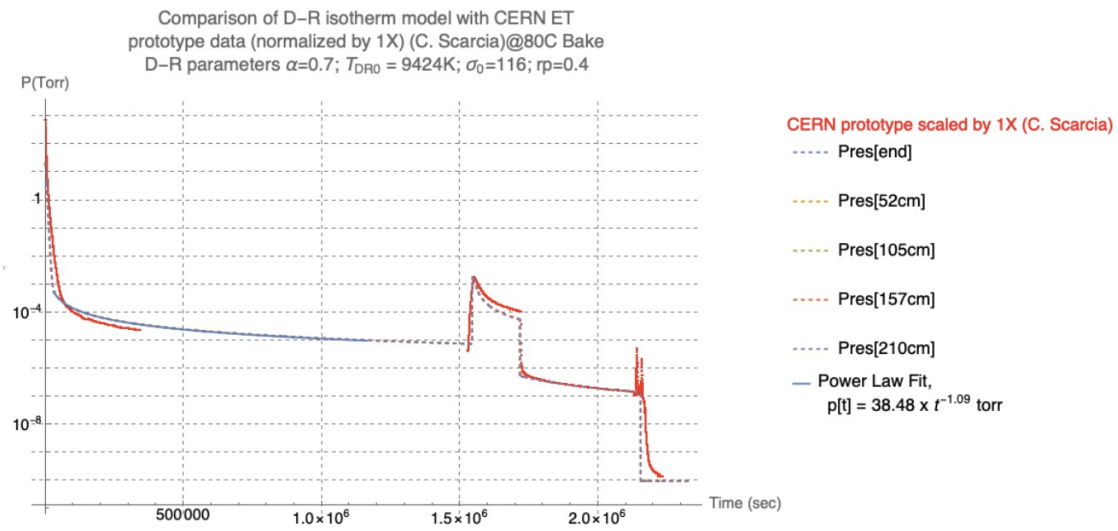

Figure 4: *Comparison of the D-R isotherm model with the CERN prototype data (data kindly shared by C. Scarcia). The data comparison allowed tuning of the D-R parameters that determine the outgassing rate. A multi-week pumpdown at room temperature is followed by a 2 day 80C bake with one pumping rate, that then is increased on day 2 of the bake for the remaining 5 days. The pressure plummets when the tube is returned to room temperature. The chamber is a cylinder 2.1m long x 0.4 m in diameter, constructed of thin-walled corrugated ferritic stainless steel and is smooth-walled. The chamber is pumped from one end; pumping is orifice-limited (1mm and 10mm options) to scale to an ET configuration - S(H_2O)= 0.117 and 11.7 l/s.*

3.1.2 LTREX data comparison

Using the same parameters that were found for the CERN data the LTREX room temperature pumpdown curve is show in the left panel of Fig. 6. The quality of the fit can be noticeably improved by adjusting the two D-R parameters (i) characteristic temperature of the binding energy distribution function of surface sites, and (ii) reservoir of H_2O on the metal surface at the start of the bake; this is modeled by an effective number of monolayers. The improved fit is shown in the right panel.

3.2 Modeling a sequential bakeout section by section.

Sequential bake without convection

The D-R model was modified to allow scenarios in which different parts of the beamtube are at different temperatures. The motivation for this is a concept for baking out extremely long beamtubes (ET, CE scale) using a sequential process that moves a localized (e.g., O[1m]) heated section of tube from one end to the other while flowing a dry inert gas (e.g., air or N_2) at low density and velocity down the tube. The idea is that the dry moving gas would entrain the outgassed H_2O vapor and move it down the tube, precluding it from back diffusing back into the section of tube that has already been baked.

A test scenario has been explored that has the following parameters.

- A mild steel tube 4" x 20' – this will be set up in the Caltech Synchrotron facility.

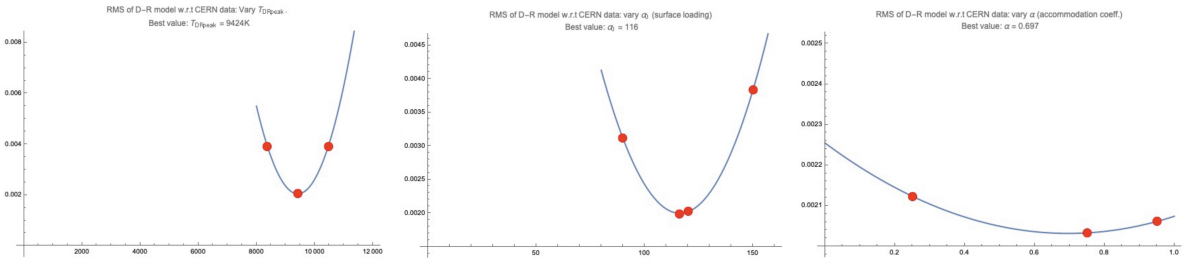

Figure 5: *Fitting the CERN data in Fig.4 leads to optimal values of the parameters $T_{DR-peak}$, σ_0 (number of effective monolayers at start of the bakeout), and α (accommodation coefficient). Vertical axis is the RMS of the factional deviation between the CERN prototype data and the D-R model for the two regions totaling 7 days during the 80C bakeout period.*

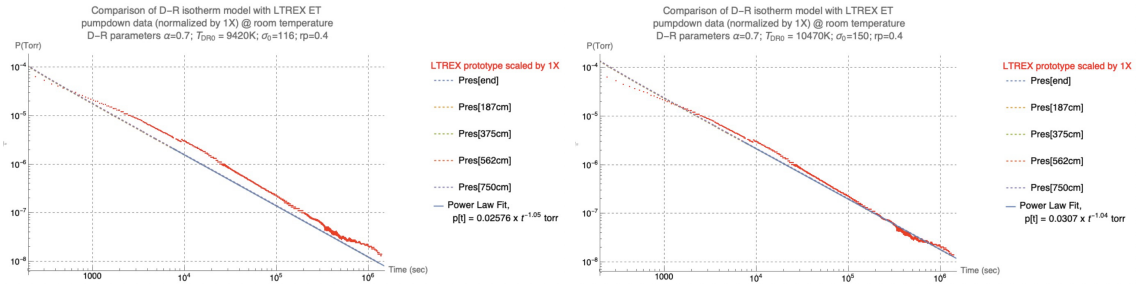

Figure 6: *Comparison of the D-R isotherm model with the LTREX room temperature pumpdown data. Left panel: model calculation using the same parameters the were optimized for the CERN data. Right panel: fit after re-tuning of the D-R parameters $T_{DRpeak}(9424K \rightarrow 10470K)$ and $\sigma_0(116 \rightarrow 150)$. The differences in material (CERN – ferritic stainless steel vs. LTREX – austenitic 304L) and surface preparation (cold-rolled/smooth vs. hot-rolled/rough and air-baked) plausibly account for the differences in the H_2O binding energy and surface loading before pumping.*

- End pumping with turbos, 160 l/s.
- 40 × 6" segmentation for the modeling.
- D-R parameters from the fit to the CERN prototype data were used.
- Each segment is baked at 150C for 6 hours, constituting a 10 day sequential bake.
- Continued pumping at room temperature (27C)followed for another 5 days.

Fig. 7 shows the initial site population occupation vs. binding energy distribution along the 40 sections of the tube. The (lower/upper) limits on the binding energy are determined by the bake temperature, the characteristic D-R isotherm distribution temperature, T_{Dpeak}, and (minimum/maximum) emission times for the H_2O molecules leaving the surface sites (see ref. [1] for details of the adaptation of the D-R isotherm model to simulation of LIGO beamtube pumping).

As the sectional bakeout proceeds the depopulation of the least bound sites progresses down the beamtube. Fig. 8 shows a snapshot about halfway through the 10-day bakeout. The depopulation of the beamtube sections 1–20 is evident.

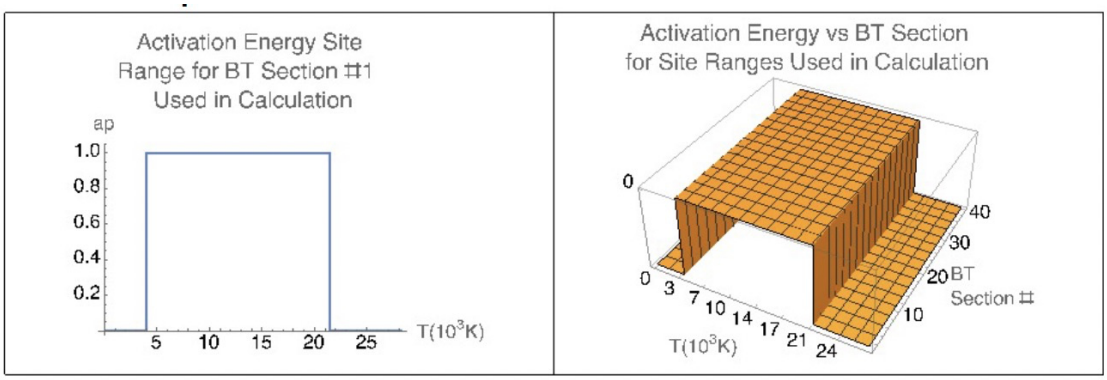

Figure 7: *Initial population probability distribution for the D-R isotherm: all sites are fully occupied from a nominally low binding energy to a sufficiently high one to ensure a bakeout does not depopulate levels at that binding energy.*

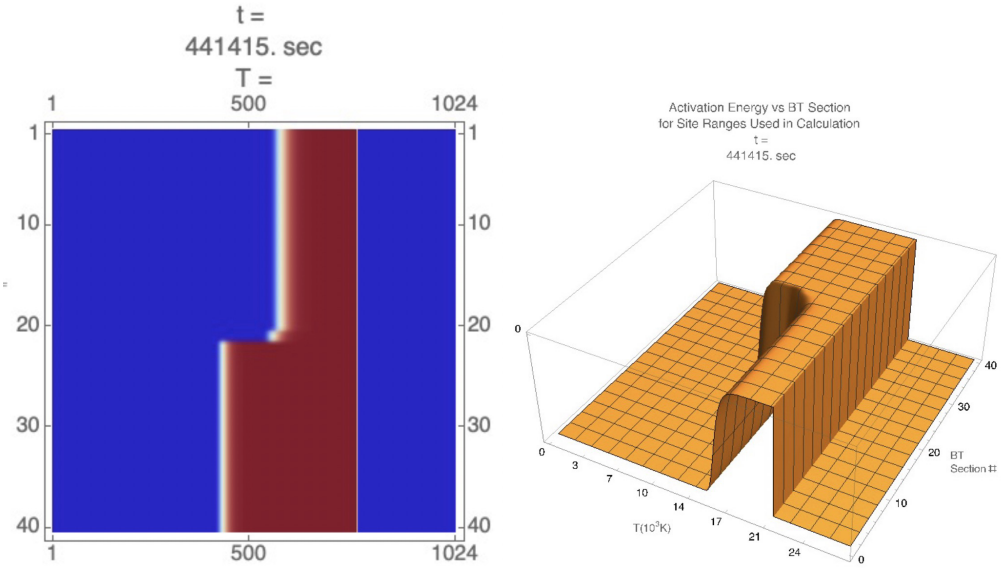

Figure 8: *A snapshot at $t = 4.4 \times 10^5$ seconds of the site occupation, ap(t,x). At this point about $\frac{1}{2}$ the tube has been baked and the corresponding lower binding energy sites for that part of the tube have become depopulated. Left panel: the ordinate is given by tube segment number (1-40) and the abscissa is site number (1-1024, $\propto kT$); refer to left panel of Fig. 3). Right panel: isometric view with axes $E \propto kT$ and Section #. These correspond to the full 40-section pumpdown shown in Fig.9.*

Four scenarios were investigated. In all cases the duration of the calculations is a total of 15 days and in all bakeout cases a particular section of tube sees an elevated temperature for 0.25 days:

Case 1 : Baseline calculation of a 15-day room temperature (27C) pumpdown.

Case 2 : The entire beamtube is baked in a conventional manner for 0.25 days at 150C then pumped for 14.75 days at room temperature.

Case 3 : A sequential bakeout of only the first 5 sections of beamtube for 0.25 days each at 150C while the rest of the tube is left unbaked. Afterwards the entire beamtube is

pumped at room temperature for another 13.75 days.

Case 4 : A sequential bakeout of all 40 sections of beamtube, each bakeout lasting 0.25 days. Afterwards the entire beamtube is pumped at room temperature for 5 days.

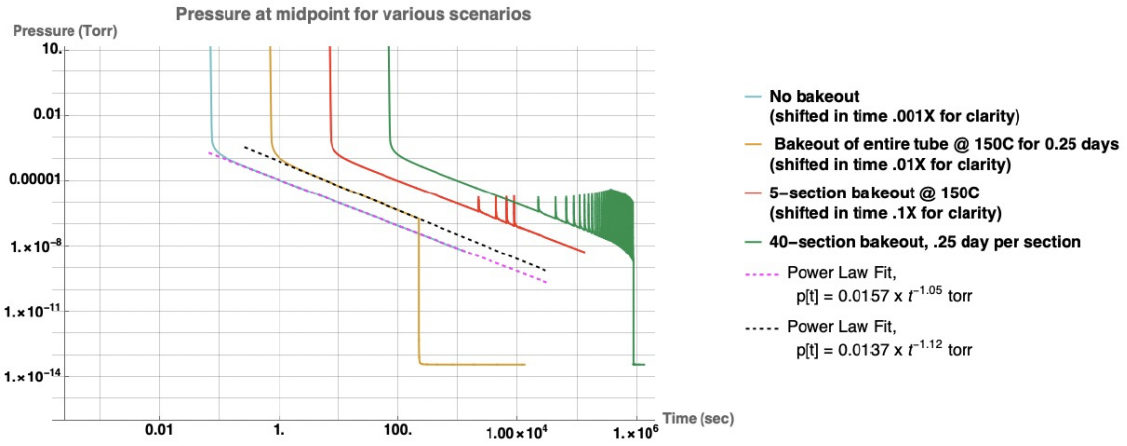

Figure 9: *Calculated p vs.T for the planned 4" x 20' mild steel demonstration at Caltech to explore sectional inductive bakeout. The four curves showing different scenarios have been offset from each other in time for ease of viewing by scaling the time axis by factors .1X, .01X, and .001X relative to the unscaled curve (otherwise the* $\sim \frac{1}{t}$ *trends would overlie one another). In all cases the system is end-pumped with two turbopumps each having a nominal speed for* H_2O *of 160 l/s. The tube is segmented into 40×6" zones(segments) where the PDE is calculated. The starting pressure was set to 20 Torr. The pressure along the tube is parabolic; shown is the pressure at the midpoint. Behavior of the curve labeled "No bakeout" (scaled by* $1/1000\times$*) shows pumpdown curve for a room temperature bakeout lasting 15 days. The curve labeled "Bakeout of entire tube" (scaled by* $1/100\times$*) shows the trend when the entire tube is baked at 150C for 0.25 days, followed by a 14.75 day room temperature pump. The curve labeled "5-section bakeout" (scaled by* $1/10\times$*) shows the trend when only the first 5 sections of tube are baked at 150C for a bake time of* $1/4$ *day per section, after which the tube is pumped down at room temperature for 13.75 days. The unscaled curve labeled "40-segment bakeout" shows the trend for the scenario in which each of the 40 6" segments is baked out sequentially over a* $40 \times 1/4$ *day period, followed by 5 days of pumping at room temperature.*

Fig. 9 presents preliminary exploratory results. Cases 1, 2, and 3 are shifted to the left for clarity of presentation. Their times were scaled by factors by $1/10\times$, $1/100\times$ and $1/1000\times$ respectively to allow them to be viewed without overlap; otherwise the curves would overlie one another. Starting at the left, Case 1 exhibits the expected monotonic $\sim 1/t$ asymptotic behavior. Next, Case 2 shows the expected pumpdown and steep drop off after returning to room temperature. The third curve, Case 3, exhibits pressure spikes at the start of sectional bakeouts and subsequent H_2O depletion of the of those sections. Because most of the tube is unbaked, the overall pumpdown behavior is essentially the same as that for the unbaked tube. Finally, Case 4 shows that at once the tube is returned to room temperature at the end the pressure drops by 5 orders of magnitude. Indeed the final pressure is essentially the same as the conventional bakeout of Case 2. It appears to be the case that a sequential bakeout is effective at removing water from the tube: the back diffusion of H_2O into the baked sections as the bake proceeds down the tube is not sufficient to cause an increase of

H_2O pressure after the bake. It seems that the depletion of occupied sites during the 150C is extensive enough that those H_2O molecules that make their way back into the baked sections fill the highest energy sites and thus remain tightly bound. This is similar to the findings by R. Weiss in his reanalysis in 2008 of the initial LIGO beam tube vacuum (ref. technical note T080330, found in [1]). Upcoming tests at Caltech will allow us to confront the modeling with data.

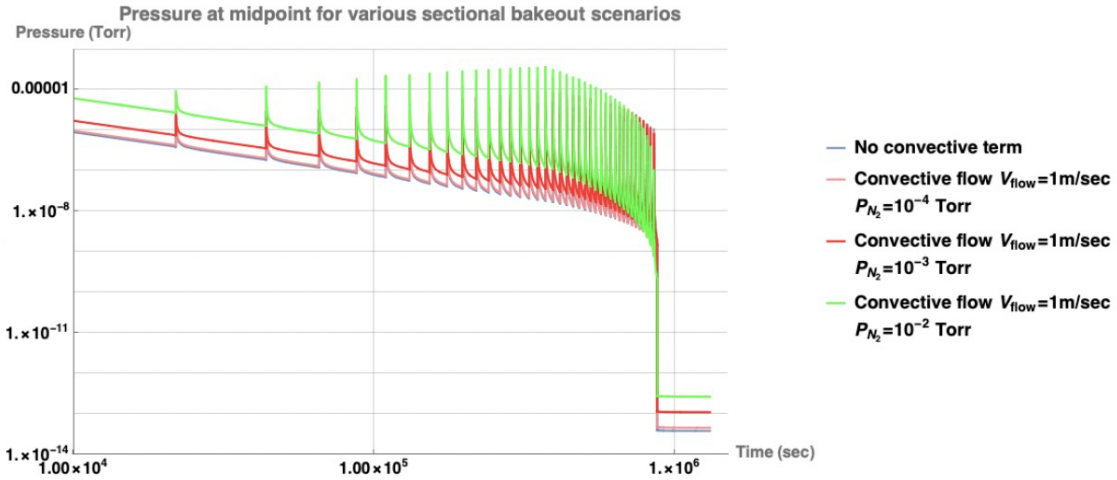

Figure 10: *Calculated p vs.T for the planned 4" x 20' mild steel demonstration at Caltech to explore sectional inductive bakeout. In all scenarios the 40 6" segments are baked out sequentially at 150C over a 10 day period, followed by 5 days of pumping at room temperature. The curve labeled "no convective term" corresponds to Case 4 in Fig. 9. It is evident that as the N_2 carrier gas background pressure is increased, the pressure of H_2O vapor in the tube increases. Refer to the text for further details.*

Sequential bake with convection

The full 40-section sequential bakeout scenario was explored with the convection term included using $V_{N_2} = 1$ m/sec at $P_{N_2} = \{10^{-2}, 10^{-3}, 10^{-4}\}$ Torr for the dry, inert carrier gas. Fig. 10 shows the results compared to Case 4 above which did not include a convective term. The results indicate a trend to higher final H_2O pressures with increasing background N_2 pressure.

It appears that with increased N_2 pressure the diffusion constant, $D(T)$ (refer to Eq. 1), decreases with increasing N_2 concentration since the diffusion constant depends on the partial pressures of both N_2 and H_2O . As it decreases, the efficacy of diffusion to disperse the H_2O vapor down the tube becomes dramatically reduced — the gas cannot reach the pumps fast enough to be depleted, and consequently the pressure in the tube builds up. Further investigation is needed to assess whether the method can work be made to work by tuning the parameters of the convection process. It seems that in order to be effective, the flow velocity of N_2 carrier gas would need to be increased substantially to make up for the dimished efficacy of molecular-flow diffusion. Referring again to Eq. 1, the trade off between the term $D(T)\nabla_x^2 p(x,t)$ and $V\nabla_x p(x,t)$ needs to be explored.

The preliminary conclusion is that adding a low-flow velocity carrier gas to entrain and remove the outgassing H_2O may be difficult to implement without extremely high carrier

gas flows (and subsequent volume of this gas).

References

[1] R. Weiss (LIGO Laboratory), *Water Outgassing Data and Model for the LIGO Beam Tubes*, https://dcc.ligo.org/LIGO-T080330, https://dcc.ligo.org/LIGO-T940090 (cit. on pp. 5, 8, 12, 15).

[2] R. Weiss (LIGO Laboratory), *Waterbake source code*, https://dcc.ligo.org/LIGO-E1600063 (cit. on p. 5).

[3] J. Feicht and A. Lazzarini (LIGO Laboratory), *Code repository in the DCC*, https://dcc.ligo.org/LIGO-E2300378, 2023 (cit. on p. 5).

[4] L. Lund and A. S. Berman, *Flow and Self-Diffusion of Gases in Capillaries. Part I*, J. Appl. Phys. 37, 2489-2495, 1966 (cit. on p. 6).

[5] M. Smoluchowski, *Über Brownsche Molekularbewegung unter Einwirkung äußerer Kräfte und den Zusammenhang mit der verallgemeinerten Diffusionsgleichung*, Ann. Phys., 4. Folge., 48, 1103–1112, 1915 (cit. on p. 8).

[6] K. Schulten and I. Kosztin (Department of Physics and Beckman Institute University of Illinois at Urbana–Champaign), *PHYS498 Lecture Notes*, https://www.ks.uiuc.edu/Services/Class/PHYS498/LectureNotes/chp4.pdf, 2000 (cit. on p. 8).

[7] WikiPedia, *The Convection–diffusion equation*, https://en.wikipedia.org/wiki/Convection–diffusion_equation (cit. on p. 8).